Polythiophenes as emitter layers for crystalline silicon solar cells: Parasitic absorption, interface passivation, and open circuit voltage

M. Zellmeier,[1] T. J. K. Brenner,[2] S. Janietz,[3] N. H. Nickel,[1] and J. Rappich[1]
[1]*Helmholtz-Zentrum Berlin für Materialien und Energie GmbH, Institut für Silizium Photovoltaik, Kekulèstr. 5, 12489 Berlin, Germany*
[2]*Institute of Physics and Astronomy, University of Potsdam, Karl-Liebknecht-Straße 24-25, 14476 Potsdam-Golm, Germany*
[3]*Fraunhofer-Institut für Angewandte Polymerforschung (IAP), Abteilung Polymere und Elektronik, Geiselbergstr. 9, 14476 Potsdam, Germany*

(Received 26 September 2017; accepted 23 December 2017; published online 16 January 2018)

We investigated the influence of the emitter (amorphous-Si, a-Si, or polythiophene derivatives: poly(3-hexylthiophene), P3HT, and poly(3-[3,6-dioxaheptyl]-thiophene), P3DOT) and the interface passivation (intrinsic a-Si or SiO_X and methyl groups or SiO_X) on the c-Si based $1 \times 1\,cm^2$ planar hybrid heterojunction solar cell parameters. We observed higher short circuit currents for the P3HT or P3DOT/c-Si solar cells than those obtained for a-Si/c-Si devices, independent of the interface passivation. The obtained V_{OC} of 659 mV for the P3DOT/SiO_X/c-Si heterojunction solar cell with hydrophilic 3,6-dioxaheptyl side chains is among the highest reported for c-Si/polythiophene devices. The maximum power conversion efficiency, PCE, was 11% for the P3DOT/SiO_X/c-Si heterojunction solar cell. Additionally, our wafer lifetime measurements reveal a field effect passivation in the wafer induced by the polythiophenes when deposited on c-Si. *Published by AIP Publishing.*
https://doi.org/10.1063/1.5006625

INTRODUCTION

The field of hybrid conducting polymer/silicon solar cells has been attracting an increasing amount of scientific attention over several years.[1,2] The main reason is the potential for cost efficiency due to the adaption of low cost solution processing to the established silicon wafer technology processes. Furthermore, promising power conversion efficiencies have been obtained for Si/poly(3-hexylthiophene) (P3HT),[3] poly(3-[3,6-dioxaheptyl]-thiophene) (P3DOT)[4] or Si/poly(3,4-ethylene-dioxythiophene):polystyrene sulfonate (PEDOT:PSS)[5–7] planar hybrid heterojunction solar cells. These results lead to a lively interest among the photovoltaic community. Similar to other heterojunctions, e.g., inorganic amorphous silicon/crystalline silicon (a-Si/c-Si) cells, the interface plays a crucial role in the device performance. The low interface recombination rate of the light induced charge carriers by passivating the Si surface improves the short circuit current and the open circuit voltage. The passivation quality is usually dependent on two parameters:[8] (i) the dangling bond density, where an increase leads to an increase in the interface recombination rate and (ii) the charge density at the interface, which is related to the magnitude of the electric field and consequently, the field effect passivation quality. This paper addresses the interface characterization of differently passivated c-Si/P3HT solar cell devices by means of spectroscopic techniques like photoluminescence (PL), surface photovoltage (SPV), and absorption measurements. The results are compared for similarly prepared planar amorphous silicon/crystalline silicon (a-Si/c-Si) solar cell reference devices. Within the a-Si:H/c-Si cell types, two different passivation methods are used to identify the influence of chemical passivation, field effect passivation and parasitic absorption at the interface on the inorganic a-Si:H/c-Si heterojunctions. These results are compared with those of the hybrid devices, and conclusions about the influence of the interface in these devices are drawn.

EXPERIMENTAL

All devices in this study were prepared from planar n-type c-Si(100) wafers with a phosphorus doping density of $N_D = 10^{15}\,cm^{-3}$. A back surface field (BSF)[9] was employed at the back side of the wafer covered by a 1 μm thick Al contact. Amorphous silicon layers were deposited using chemical vapour deposition (CVD) techniques.[10] P3HT layers were spin coated under a N_2 atmosphere in a glove box. The oxygen and water values were kept below 0.1 ppm. Surface passivation of the silicon crystals was performed by either a SiO_X tunneling oxide (native oxide), H-termination (5 min dip in 5% HF solution), or via electrochemical methylation[11] from methyl-Grignard (CH_3-MgBr). For the native oxide, the H-terminated samples were stored in clean room air for 12 h.

For amorphous/crystalline (a-Si/c-Si) reference devices, a 13 nm thick p-type a-Si emitter was deposited either on the SiO_X passivated c-Si surface or on a 5 nm thick intrinsic amorphous silicon interlayer (i-a-Si) with additional hydrogen treatment.[12–16] The use of this i-a-Si interlayer led to the best a-Si/c-Si heterojunction solar cells due to excellent passivation properties.[8]

For hybrid devices, high molecular weight regioregular (rr) P3HT, as purchased from Ossila, and P3DOT were dissolved in 1,2-dichlorbenzene and spin coated as follows: 1 mg/ml at 2000 rpm for the hydrophilic oxide surface and 3 mg/ml at 2200 rpm for the hydrophobic H- or CH_3-termination. The P3HT and P3DOT layers were additionally covered

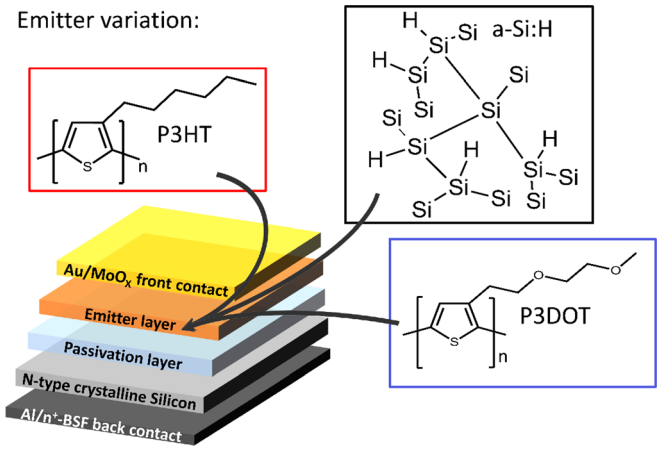

FIG. 1. Sketch of the device structure with different emitter materials used in the emitter variation study.

by a 5 nm thick layer of MoO_3 to avoid shunting of the polymer,[4] and finally a 12 nm thick semi-transparent Au layer was used as a front contact. For consistency, the same contact system was used for the inorganic solar cells. Both layers were deposited by thermal evaporation at a base pressure of 10^{-7} mbar. A sketch of the resulting devices with different emitter layers is depicted in Fig. 1.

The absorption spectra were determined measuring the absorption and transmission spectra separately,[17] using a Perkin Elmer UV/Vis Lambda 1050 spectrometer. The spot size was chosen to be smaller than the active area size and focused fully on the solar cell.

Photoluminescence (PL)-measurements were conducted exciting the sample using short laser pulses (3 ns) at 365 nm and measured at 1130 nm (bandgap of Si).

Device efficiencies were determined under AM 1.5G conditions. The cell size was $1 \times 1\,cm^2$. External quantum efficiency (EQE) measurements were performed under short circuit conditions using chopped, monochromatic light and a lock-in amplifier with additional white light illumination to increase the charge carrier density closer to working point conditions.

The effective minority charge carrier lifetime of the prepared structures was quantified by means of photoconductance decay measurements on a WCT-100 system (Sinton Instruments).[18] The samples for the lifetime measurements were whole 4-in. wafers with a BSF. The front side of these wafers was fully covered with the polymer by spin coating, as mentioned above. Please note that no MoO_X/Au contact scheme was used for the measurements.

Surface photovoltage (SPV) measurements were conducted[19] to quantify the c-Si band bending in equilibrium. For the sample excitation, a pulsed 900 nm laser was used. All measurements were performed in ambient air. Again, no contacts were applied.

RESULTS AND DISCUSSION

Surface photovoltage and photoluminescence investigation

Figure 2(a) presents the density of interface defects, D_{it}, for three different interface terminations commonly used in

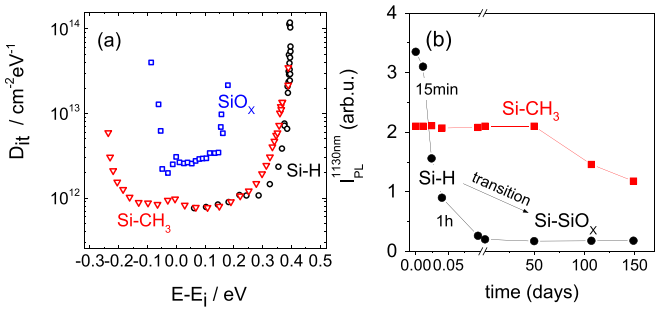

FIG. 2. (a) Interface state density D_{it} of c-Si(100) for different surface treatments determined by SPV; (b) PL intensity recorded at 1130 nm of H- and CH_3-terminated Si(111) surfaces as a function of time in ambient air.

hybrid solar cells (HSCs), as measured by SPV.[20,21] The low defect density of the H-termination (open circle) achieved by an HF-Dip was maintained by electrochemical grafting of CH_3 groups (open triangle) using a Grignard reagent.[11] The D_{it} of a passivating thin tunneling oxide (open rectangle) is about a factor of 4 higher. The long time stability of the CH_3-termination of c-Si is shown in Fig. 2(b) in comparison to an H-terminated c-Si surface measured by PL as a function of time in ambient air. The CH_3-termination shows no change in the PL-intensity and is stable for more than 50 days until it starts to decay at longer times in ambient air. The PL intensity of the H-terminated c-Si surface is slightly higher in the beginning, but the PL of the H-terminated c-Si surface decays within 2 h under the same environmental conditions and turns into a SiO_X passivated state. This formed SiO_X/c-Si interface had more than a factor of 10 higher defect concentration compared to the CH_3-terminated Si surface.

Nevertheless, besides surface passivation, the wetting behavior of the surface is a matter of particular interest for spin-coating processes, since oxides are hydrophilic and H- or CH_3-terminated Si surfaces are hydrophobic.[22,23] This will lead to different P3HT layer thicknesses and/or layer structures that will influence the device performance as discussed in the next paragraphs.

Absorption and external quantum efficiencies

Figure 3(a) shows the absorption spectra of hole conducting layers of 13 nm p-type a-Si and 15 nm P3HT on a glass substrate. The absorption of P3HT starts at about 1.9 eV, which shows a maximum at 2.2 eV and decays towards higher energies. The absorption of a-Si starts at about 1.71 eV (E_g(a-Si)), outperforms that of the P3HT at about 2.3 eV, and finally increases with increasing light energy due to the direct proportionality of transition probability to the density of states in valence and conduction bands.[24]

The difference in the absorption of the emitter layer and the variation of the interface has led to significant changes in the spectral response of the external quantum efficiency (EQE) data, as presented in Figs. 2(b) and 2(c). The EQE is enhanced in the short wavelength region due to reduced absorption of SiO_X compared to the intrinsic a-Si (i-a-Si) layer in the a-Si/c-Si solar cell structure [see Fig. 2(b)]. A strong research interest is directed towards taking advantage

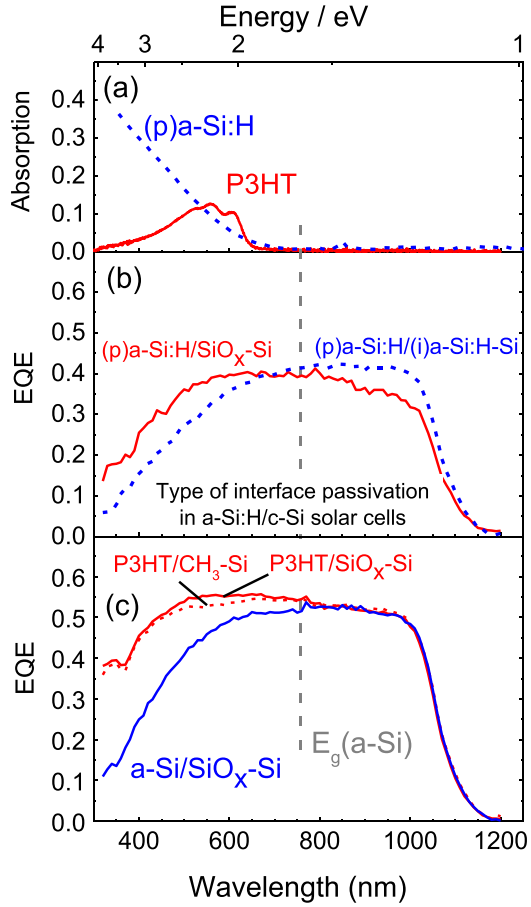

FIG. 3. (a) Absorption spectra of 13 nm p-type a-Si (dashed line) and 15 nm P3HT (solid line) on glass substrates, (b) external quantum efficiencies (EQEs) of a-Si:H/c-Si heterostructure solar cells with intrinsic a-Si (i-a-Si, dashed line) and SiO_X passivation (solid line) layers, and (c) EQE of P3HT/SiO_X/c-Si, a-Si/SiO_X/c-Si (solid lines), and P3HT/CH_3-Si (dashed line) solar cells.

of the high transparency of SiO_X.[25,26] A reduced EQE in the long wavelength regime is mainly a result of the significantly better passivation of the i-a-Si/c-Si interface than that of the SiO_X/c-Si interface. This behavior is also reflected by the EQE measured for the SiO_X interface passivation [see Fig. 3(c)] in the P3HT/SiO_X/c-Si and a-Si/SiO_X/c-Si cells, respectively. Additionally, the CH_3-terminated Si surface in the P3HT/CH_3/c-Si solar cell device shows a slightly reduced EQE in the spectral range in which P3HT absorbs, and is a result of higher absorption by the thicker P3HT layer (~34 nm) on the hydrophobic CH_3 surface compared to that prepared on the hydrophilic SiO_X surface (~15 nm).

Table I compares the emitter thickness, the type of interface passivation, the open circuit potential (V_{OC}), the short circuit current (j_{SC}), the fill factor (FF), and the power conversion efficiency (PCE), as measured for different types of solar cells. As expected, j_{SC} is higher for the P3HT/c-Si devices than for the a-Si/c-Si devices due to the significantly stronger absorption of the a-Si layer compared to P3HT in the lower wavelength range [see Fig. 3(a)]. The relative low PCE of 8% for the a-Si/i-a-Si/c-Si solar cell is a result of the planar structure without any light trapping scheme, and consequently a low short circuit current of only 18.1 mA cm^{-2}, as used for all devices presented in this study. The thicker P3HT layer in the P3HT/CH_3/c-Si solar cell led to a much smaller FF than for the thinner layer in the P3HT/SiO_X/c-Si device due to the higher resistance loss. Nevertheless, the P3HT/c-Si hybrid solar cell structures exhibit a PCE of about 10%.

The highest V_{OC} was obtained for the a-Si/i-a-Si/c-Si solar cell with about 670 mV due to the very good passivation by the hydrogenated i-a-Si interface, whereas the lowest V_{OC} was measured for the SiO_X interface which led to the highest defect concentration at the c-Si interface (see Fig. 2). Surprisingly, the P3HT containing solar cells had a V_{OC} above 610 mV, independent of the passivation layer used.

Lifetime measurements and influence of partial charge in the polymer

The high V_{OC} for Si in combination with P3HT is probably connected to the blocking of majority charge carriers at the Si/gold interface. These influences have been investigated by lifetime measurements on c-Si wafers with a-Si passivation on the backside and oxide passivation on the front side. The measured lifetime, τ_{15}, at a photogenerated minority carrier density equal to the doping level of c-Si was 19.6 μs and increases to 37.5 μs after deposition of P3HT on the SiO_X interfacial passivation layer of the very same c-Si wafer. This increase of τ_{15} after spin coating of the polymer is accompanied by an increase in the dark band bending, as measured by SPV (from −47.1 meV to −65.9 meV). Both results confirmed a field effect passivation effect[27] by the spin coated P3HT onto the SiO_X interlayer probably due to a positive charge induced in the n-type c-Si wafer by the negatively charged π-electron system of the polymer.

Furthermore, the effective c-Si lifetime is correlated to the so-called implied open circuit voltage (iV_{OC}), which is the maximum possible V_{OC} that can be obtained when only

TABLE I. Comparison of emitter thickness, type of interface passivation, open circuit potential (V_{OC}), short circuit current (j_{SC}), fill factor (FF), and power conversion efficiency (PCE), as measured for different types of inorganic and hybrid planar c-Si based heterojunction solar cells with a MoO_X/Au front contact system on a 1 × 1 cm^2 active area.

Cell type	Emitter thickness (nm)	Interface passivation	V_{OC} (mV)	j_{SC} (mA/cm^2)	FF (%)	PCE (%)
a-Si/c-Si	13 ± 1	(i) a-Si:H	669	18.1	66.3	8.0
a-Si/c-Si	13 ± 1	SiO_X	558	16.4	62.4	5.6
P3HT/c-Si	15 ± 2	SiO_X	612	19.8	83.1	10.1
P3HT/c-Si	34 ± 3	CH_3	617	20.6	72.6	9.2
P3DOT/c-Si	18 ± 2	SiO_X	659	22.1	75.7	11.0

recombination is the main loss process for charge carriers. The V_{OC} for the a-Si/c-Si device with an oxide interface passivation is 558 mV (see Table I). The result is in good agreement with the value measured for the implied open circuit voltage $iV_{OC} = 570$ mV obtained for the silicon oxide interface passivation at one sun. Additionally, these values for iV_{OC} are in agreement with the measured lifetimes of $\tau_{15} = 19.6$ μs (see Fig. 4).[28,29] The lifetime does not significantly increase for lower charge carrier injection densities. At one sun, a charge carrier injection density of 4.2×10^{14} cm^{-3} is determined, which corresponds to a slightly higher lifetime of 21.2 μs. The field effect passivation induced by the P3HT, however, is too little to explain the high V_{OC} of the P3HT/SiO_X/c-Si devices. Especially, in the case of the P3HT/c-Si heterojunctions, only a negligible influence of the interface passivation layer on the surprisingly high V_{OC} was observed (see Table I). These results do not reflect the typical behavior known for a-Si/c-Si heterojunction solar cells, whose performance strongly depends on the quality of the interface passivation.[30] Moreover, the interface passivation independent V_{OC} of the P3HT/c-Si devices suggests a structural dependence of V_{OC} in such devices. Sheng *et al.*[6] found an improvement of their devices based on different preparation methods of the intrinsic SiO_X interlayer, which is ascribed to the stronger wettability due to increased roughness and hydrophilicity.

Therefore, a P3HT derivative with hydrophilic oxygen atoms in the side chain (poly(3-[3,6-dioxaheptyl]-thiophene), P3DOT,[31] was used to investigate the influence of the wettability and the structural quality of the spin coated layer. The structure of P3DOT is shown in Fig. 5 together with the current-voltage curve of the c-Si/SiO_X/P3DOT device measured under AM 1.5G conditions. The increase in the PCE to about 11% compared to that of the c-Si/SiO_X/P3HT device is partly due to an increase in V_{OC}. Please note that neither the band bending (−36.1 meV) nor the effective c-Si wafer lifetime ($\tau_{15} = 26.5$ μs) is connected to this higher performance, since they are both lower than those of the P3HT/SiO_X/c-Si device. The open circuit voltage of 659 mV is comparable to those of optimized a-Si/c-Si solar cells and, to our knowledge,

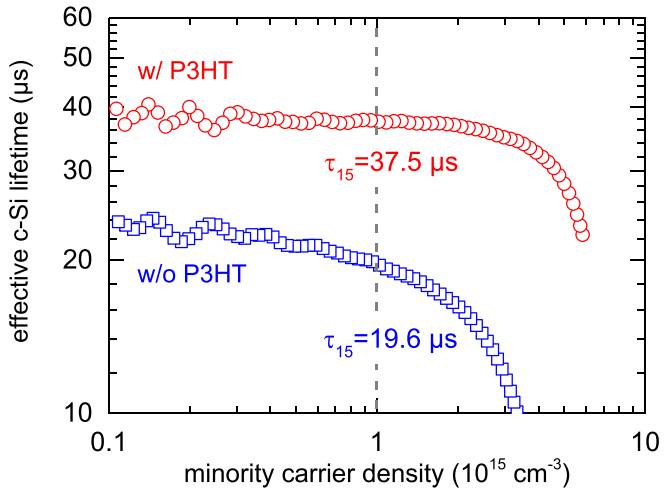

FIG. 4. Effective wafer lifetime of the same SiO_X passivated n-type c-Si wafer with and without a spin coated layer of P3HT.

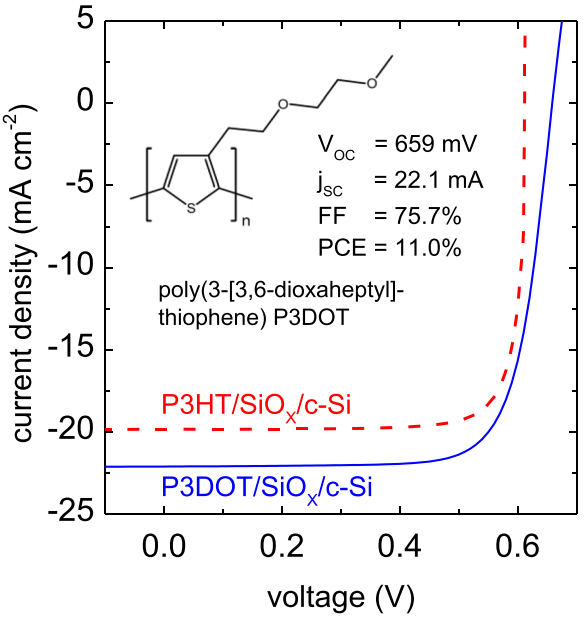

FIG. 5. Current-voltage curve of the P3DOT/SiO_X/c-Si and P3HT/SiO_X/c-Si solar cell devices measured under AM 1.5G conditions. Insert: Structure of poly(3-[3,6-dioxaheptyl]-thiophene), P3DOT, and data for the solar cell characteristics of the P3DOT/SiO_X/c-Si device (see also Table I).

is among the highest for c-Si based hybrid solar cells reported so far.[32]

Structural dependence as well as reduced influence of surface states was reported by Green.[33] He concluded that dynamic effects of the surface states are generally negligible for MIS devices with an inversion layer at the interface. Also, surface defect states higher than 10^{13} cm^{-2} may be tolerated without significantly diminishing the device performance. The reason for that can be understood by the following consideration: The pn-junction of inversion layer devices is formed within the silicon in close proximity to the surface and thereby reducing the influence for surface states. The charge separation has already occurred in the bulk of the semiconductor. Formation of an inversion layer at the silicon/organic interface has already been reported in combination with PEDOT:PSS.[34,35] However, we do not observe this behavior with P3HT. The band bending for P3HT as well as for P3DOT is too small and amounts to less than 100 meV. The inversion of the silicon is rather caused by the MoO_X/Au front contact. Again, SPV measurements were used to determine the influence of every single front side layer in the solar cell. Figure 6 itemizes the results of the measurements for a P3HT emitter. Additionally, the thresholds for inversion and strong inversion are marked. Inversion is defined as $V_{BI} > E_F$-E_I. For strong inversion, the relation changes to $V_{BI} > 2|E_F$-$E_I|$ and depends, due to the energetic position of the Fermi energy, on the Si doping density. The use of MoO_X layers on P3HT and SiO_X leads to an increased band bending that moves close to the strong inversion threshold. The result is not surprising as MoO_X is under investigation as a low absorption emitter for silicon.[36] The addition of the gold layer leads to a reduction of the measured band bending. However, this is due to a restriction of the measurement method. The additional gold layer absorbs too much

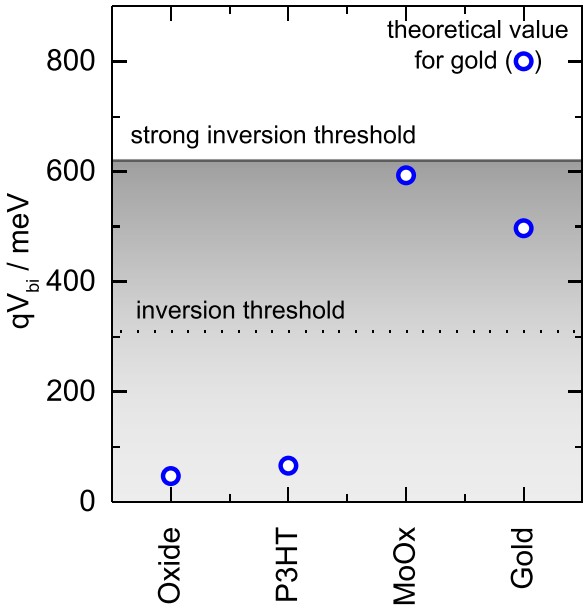

FIG. 6. Development of the band bending in hybrid solar cells for deposition of the individual functional front layers.

light intensity of the 900 nm laser. As a consequence, the prerequisite for the flat band condition in the silicon upon illumination is not satisfied and V_{Bi} is underestimated. On this account, two measures were taken to estimate the error introduced by the measurement method. In Fig. 6, the theoretical value for gold according to Schottky theory for a gold work function of $WF_{Au} = 5.2\,eV$ is added. This value is expected to overestimate the barrier height. For one, a typical value for a naturally passivated gold surface is probably lower.[37,38]

This observation suggests that a metallic state of the organic material is a prerequisite for the formation of the inversion layer in silicon and consequently high efficiency hybrid solar cells.

CONCLUSIONS

We investigated the influence of the emitter (a-Si or polythiophene derivatives, P3HT and P3DOT) and the interface passivation on the c-Si based planar heterojunction solar cell parameters on the $1 \times 1\,cm^2$ active area. We found higher short circuit currents for the P3HT or P3DOT/c-Si solar cells than those obtained for a-Si/c-Si devices, independent of the interface passivation. This observation is due to the narrow absorption region of P3HT/P3DOT, which reduces the parasitic absorption in the wavelength region below 700 nm compared to a-Si.

Furthermore, the independence of the passivation quality of the intrinsic interlayer, which is in contradiction to the theory for standard silicon heterojunctions, and different wettability properties of the passivation layers, suggest a structural dependence of the better planar hybrid/c-Si device performance. This was confirmed by exchanging the hydrophobic hexyl side chains of P3HT by hydrophilic 3,6-dioxaheptyl side chains. The resulting P3DOT/SiO_X/c-Si heterojunction solar cell led to a higher hybrid solar cell performance ($V_{OC} = 659\,mV$, $PCE = 11\%$) than that obtained using P3HT. Additionally, the V_{OC} of 659 mV is so far the highest reported value for such a type of solar cell.

ACKNOWLEDGMENTS

The Helmholtz Energy-Alliance financially supported this work. The authors would like to thank Mrs. Kerstin Jacob for wafer cleaning and Mr. Erhard Conrad for the preparation of amorphous silicon layers.

[1]W. Wang and E. A. Schiff, Appl. Phys. Lett. **91**, 133504 (2007).
[2]M. J. Sailor, E. J. Ginsburg, C. B. Gorman, A. Kumar, R. H. Grubbs, and N. S. Lewis, Science **249**, 1146 (1990).
[3]S. Avasthi, S. Lee, Y.-L. Loo, and J. C. Sturm, Adv. Mater. **23**, 5762 (2011).
[4]M. Zellmeier, J. Rappich, M. Klaus, C. Genzel, S. Janietz, J. Frisch, N. Koch, and N. H. Nickel, Appl. Phys. Lett. **107**, 203301 (2015).
[5]F. Zhang, D. Liu, Y. Zhang, H. Wei, T. Song, and B. Sun, ACS Appl. Mater. Interfaces **5**, 4678 (2013).
[6]J. Sheng, K. Fan, D. Wang, C. Han, J. Fang, P. Gao, and J. Ye, ACS Appl. Mater. Interfaces **6**, 16027 (2014).
[7]M. Pietsch, S. Jäckle, and S. Christiansen, Appl. Phys. A **115**, 1109 (2014).
[8]S. Olibet, E. Vallat-Sauvain, and C. Ballif, Phys. Rev. B **76**, 35326 (2007).
[9]J. Nelson, *The Physics of Solar Cells* (Imperial College Press, 2003).
[10]B. Stegemann, J. Kegel, M. Mews, E. Conrad, L. Korte, U. Stürzebecher, and H. Angermann, Energy Procedia **38**, 881 (2013).
[11]F. Yang, K. Roodenko, R. Hunger, K. Hinrichs, K. Rademann, and J. Rappich, J. Phys. Chem. C **116**, 18684 (2012).
[12]A. Descoeudres, L. Barraud, S. De Wolf, B. Strahm, D. Lachenal, C. Guérin, Z. C. Holman, F. Zicarelli, B. Demaurex, J. Seif, J. Holovsky, and C. Ballif, Appl. Phys. Lett. **99**, 123506 (2011).
[13]T. F. Schulze, L. Korte, F. Ruske, and B. Rech, Phys. Rev. B **83**, 165314 (2011).
[14]W. Fuhs, L. Korte, and M. Schmidt, J. Optoelectron. **8**, 1989 (2006).
[15]L. Korte and M. Schmidt, J. Non-Cryst. Solids **354**, 2138 (2008).
[16]M. Mews, T. F. Schulze, N. Mingirulli, and L. Korte, Appl. Phys. Lett. **102**, 122106 (2013).
[17]L. Schaefer and C. Bergmann, *Lehrbuch Der Experimentalphysik: Optik: Wellen- Und Teilchenoptik* (de Gruyter, 2004).
[18]R. A. Sinton and A. Cuevas, Appl. Phys. Lett. **69**, 2510 (1996).
[19]K. Heilig, Solid State Electron. **21**, 975 (1978).
[20]K. Heilig, Surf. Sci. **44**, 421 (1974).
[21]H. Angermann, T. Dittrich, and H. Flietner, Appl. Phys. A **59**, 193 (1994).
[22]R. Williams and A. M. Goodman, Appl. Phys. Lett. **25**, 531 (1974).
[23]R. G. Frieser, J. Electrochem. Soc. **121**, 669 (1974).
[24]P. Y. Yu and M. Cardona, *Fundamentals of Semiconductors: Physics and Material Properties*, 3rd ed. (Springer, 2005).
[25]M. Liebhaber, M. Mews, T. F. Schulze, L. Korte, B. Rech, and K. Lips, Appl. Phys. Lett. **106**, 31601 (2015).
[26]Z. R. Chowdhury and N. P. Kherani, Prog. Photovoltaics **23**, 821 (2015).
[27]M. Reusch, M. Bivour, M. Hermle, and S. W. Glunz, Energy Procedia **38**, 297 (2013).
[28]P. Würfel, *Physik Der Solarzellen* (Springer, 1995).
[29]C. Leendertz, "Effizienzlimitierende Rekombinationsprozesse in amorph/kristallinen und polykristallinen Siliziumsolarzellen," Ph.D. thesis, Technische Universität Berlin, Fakultät II – Mathematik und Naturwissenschaften, 2012 [in German].
[30]A. G. Aberle, Prog. Photovoltaics **8**, 473 (2000).
[31]T. Bilkay, K. Schulze, T. Egorov-Brening, A. Bohn, and S. Janietz, Macromol. Chem. Phys. **213**, 1970 (2012).
[32]J. He, P. Gao, Z. Yang, J. Yu, W. Yu, Y. Zhang, J. Sheng, J. Ye, J. C. Amine, and Y. Cui, Adv. Mater. **29**, 1606321 (2017).
[33]M. A. Green, Appl. Phys. Lett. **33**, 178 (1978).
[34]S. Jäckle, M. Mattiza, M. Liebhaber, G. Brönstrup, M. Rommel, K. Lips, and S. Christiansen, Sci. Rep. **5**, 13008 (2015).
[35]A. S. Erickson, A. Zohar, and D. Cahen, Adv. Energy Mater. **4**, 1301724 (2014).
[36]J. Ziegler, M. Mews, K. Kaufmann, T. Schneider, A. N. Sprafke, L. Korte, and R. B. Wehrspohn, Appl. Phys. A **120**, 811–816 (2015).
[37]W. Osikowicz, M. P. de Jong, S. Braun, C. Tengstedt, M. Fahlman, and W. R. Salaneck, Appl. Phys. Lett. **88**, 193504 (2006).
[38]H. Kuchling, *Taschenbuch Der Physik*, 11th ed. (Hanser Verlag, 1988).